Mean field dynamical exponents in finite-dimensional Ising spin glass

Mean field dynamical exponents in finite-dimensional Ising spin glass

G Parisi†, P Ranieri†, F Ricci-Tersenghi‡ and J J Ruiz-Lorenzo‡

Dipartimento di Fisica, Università di Roma, La Sapienza and INFN, Sezione di Roma I, P A Moro 2, 00185 Rome, Italy

Abstract. We have studied numerically the remanent magnetization in the six- and eight-dimensional Ising spin glass and we have compared it with the behaviour observed in the SK model, that we have also computed analytically. We also report the value of the dynamical critical exponent z in six dimensions measured in three different ways: from the behaviour of the energy and the susceptibility as a function of the Monte Carlo time and by studying the overlap–overlap correlation function as a function of space and time. These three results are in very good agreement with the mean field prediction $z = 4$. Finally we have checked numerically the analytical prediction, obtained by assuming spontaneously broken replica symmetry, for the most singular part of the propagator in the spin-glass phase. This last result supports the existence of spontaneously broken replica symmetry in finite-dimensional spin glasses.

1. Introduction

Two main problems in the current spin-glass theoretical research can be identified. The first is the nature of the spin-glass phase in finite dimensions. The droplet theory cannot be used to explain much of the numerical data available for the interpretation in the framework of mean field (MF) theory (i.e. with spontaneously broken replica symmetry) [1]. In the last part of this paper we will see that the numerical data point, in particular one of the propagators of the theory, clearly correspond to a low-temperature phase of the MF type.

We note that in a recent paper [2] it was shown that if the infinite volume is calculated in a given (weak) topology, the infinite volume overlap probability distribution $P(q)$ does not depend on the couplings (always in this weak-product topology). This result does not contradict our findings, which indicate the correctness of the MF expressions for the propagators.

The second problem is the analytical calculation of critical exponents (static and dynamical) in three dimensions enabling the comparison of theory with experiment. The first part of this paper is devoted to the study of the value of the upper critical dimension for the decay exponent of the remanent magnetization. This knowledge is essential for further calculation of the value of this exponent in finite dimensions (e.g. using the ϵ expansion). This exponent has great physical importance, mainly because it gives information on the early regimes of the dynamics and because it is often measured experimentally [3].

---

† E-mail address: parisi,ranieri@roma1.infn.it
‡ E-mail address: ricci,ruiz@chimera.roma1.infn.it

The remanent magnetization is defined as follows: we put the system under a large magnetic field, turn it off and follow the decay of the magnetization of the system. The magnetization decays as

$$M(t) \sim t^{-\lambda} \tag{1}$$

which defines the λ exponent [4]. Following the results of Fisher and Sompolinsky [5] we should expect that λ is equal to the MF value only for $d \geqslant 8$, i.e. for exponents of observables which are reminiscent of the 'magnetic field, the upper critical dimension is eight, not six.

Here we numerically check this fact that we have computed analytically, obtaining the value of the λ exponent in six, eight and infinite dimensions (the SK model). These results show that for this observable the upper critical dimension is eight instead of six. Moreover, we have found numerically for the SK model, that the dependence of λ with the temperature is discontinuous at the critical point.

Another related issue addressed in this paper is the numerical evaluation of the dynamical critical exponent in six dimensions. In the past Wang and Young [6] checked that in six dimensions the static critical exponent are those of MF, but such a check is still lacking for the dynamical side of the problem. Hence, another of the aims of this paper is to show that the upper critical dimension is six for dynamics as well. To do this, we have developed different techniques that yield accurate determinations of the dynamical exponent.

In further analyses we will use these techniques in five dimensions in order to check the recent analytical calculations of Parisi and Ranieri [8] who have been able to compute the one-loop correction to the dynamical critical exponent, z, whose MF value (the base of the ϵ-expansion) is 4. They found

$$z(\epsilon) = 4 \left(1 - \frac{\epsilon}{12}\right) \tag{2}$$

where $\epsilon = 6 - d$.

In particular we have obtained the z exponent [10] using three different off-equilibrium methods: the decay of the energy, the growth of the nonlinear susceptibility and the scaling of the overlap–overlap correlation function. These three methods provide us with three estimates of z or ratios of z to the static critical exponents which are in very good agreement with the MF predictions ($\nu_{MF} = \frac{1}{2}$, $\eta_{MF} = 0$ and $z_{MF} = 4$).

Whereas calculations of z have been done at the critical temperature of the system we have performed numerical simulations inside the cold phase to monitor the 'expected' dependence on the temperature of the exponent z (as obtained in three and four dimensions [11, 12]) and to check the predictions of De Dominicis *et al* [9] (by monitoring the growth of the susceptibility) that imply that the propagator restricted to the $q = 0$ ergodic component behaves like p^{-4}, where p is the momenta of the propagator. Obviously at the critical point we expect the usual dependence on the momenta, i.e. p^{-2}.

We note that the analytical prediction of De Dominicis *et al* [9] was done assuming that the spontaneous breaking of the replica symmetry is that of MF. Hence, our numerical results are a further test that the spin glasses in finite dimensions follow the picture of MF.

2. Numerical simulation and observables

We have simulated the six- (eight-)dimensional Ising spin glass (SG) whose Hamiltonian defined in a hypercube of volume L^d with periodic boundary conditions is

$$\mathcal{H} = -\sum_{\langle i,j \rangle} S_i J_{ij} S_j \tag{3}$$

where $\langle i, j \rangle$ denotes nearest-neighbour pairs, $J_{ij} = \pm 1$ (with the same probability) are quenched variables and $S_i = \pm 1$ are spin variables.

The static of this model was studied by Wang and Young [6]. Simulating lattice sizes up to $L = 8$ they found that the static critical exponents were compatible with the MF predictions ($\nu_{MF} = \frac{1}{2}, \eta_{MF} = 0$) and that there were logarithmic corrections to the MF exponents, an effect linked to the upper critical dimension. Their estimate for the critical temperature was $T_c = 3.035 \pm 0.01$.

We will study the decay of the remanent magnetization defined as

$$M(t, t_w) = \frac{1}{L^d} \sum_{i=1}^{L^d} \sigma_i(t)\sigma_i(t_w) \qquad t \gg t_w. \tag{4}$$

This observable decays as

$$M(t, t_w) \propto t^{-\lambda}. \tag{5}$$

We find that the MF prediction for this exponent is $\lambda = \frac{5}{4}$.

Another aim of this paper is to measure the dynamical critical exponent z in order to compare it with the MF results ($z_{MF} = 4$). To do this we have measured the behaviour of the energy and susceptibility as a function of the Monte Carlo time

$$E(t) - E_\infty \propto t^{-\delta} \tag{6}$$

$$\chi(t) \propto t^h \tag{7}$$

and the $q - q$ correlation function.

We will also examine the dependence of the energy on the Monte Carlo time. We assume that at the critical point (and only at the critical point) it is possible to connect the approach to equilibrium of the energy and of the equal time correlation functions to the equilibrium static and dynamical exponents. For example, in the case of the energy we find:

$$E(t) - E_\infty \propto t^{-\dim(E)/z} \qquad T = T_c \tag{8}$$

where z is the dynamical critical exponent, $\dim(E) \equiv d - 1/\nu$ is the dimension of the energy operator and d is the dimension of space. Assuming $d = 6$ and $\nu = \nu_{MF} = \frac{1}{2}$ we have that the exponent of the energy decay at $T = T_c$ is $\delta = 4/z$.

Analogously for the nonlinear susceptibility

$$\chi(t) = L^d \overline{\langle q^2(t) \rangle} \qquad q(t) = \frac{1}{L^d} \sum_i \sigma_i(t)\tau_i(t) \tag{9}$$

where σ and τ are two real replicas with the same quenched disorder, we can write the following dependence on Monte Carlo time [7]

$$\chi(t) \propto t^{(2-\eta)/z} \qquad T = T_c \tag{10}$$

for $t \ll \tau_{eq}(L)$, where $\tau_{eq}(L)$ is the equilibration time, which should diverge as $\tau_{eq}(L) \propto L^z$. Here we have used that $\dim(\chi) = 2 - \eta$. By assuming the MF value for η we obtain for the exponent of susceptibility: $h = 2/z$ at $T = T_c$.

From these formulæ it is possible to calculate the dynamical exponent via two different observables. In the six-dimensional case, if $z = z_{MF} = 4$ we should see a behaviour like t^{-1} for the energy and $t^{1/2}$ for the non linear susceptibility.

The final method of calculating the dynamical exponent is to use the overlap–overlap correlation length at distance x and time t defined by

$$G(x, t) \equiv \frac{1}{V} \sum_i \overline{\langle \sigma_{i+x}\tau_{i+x}\sigma_i\tau_i \rangle} \tag{11}$$

where again σ and τ are two real replicas with the same disorder.

In the simulations we start from a random configuration ($T = \infty$) and suddenly quench the system to T_c or below. Then the system begins to develop internal correlations and we can define a time-dependent off-equilibrium correlation length, $\xi(T, t)$, as the typical distance over which the system has already developed correlations different from zero, i.e. $G(x, t) \simeq 0$ for $x > \xi(T, t)$.

The growth of this correlation length with the Monte Carlo time defines the dynamical exponent z trough

$$\xi(T, t) \propto t^{1/z(T)}. \tag{12}$$

We have seen that in three and four dimensions [11, 12] the data fit very well the following functional form

$$G(t, x) = \frac{A(T)}{x^\alpha} \exp\left\{ -\left(\frac{x}{\xi(T, t)} \right)^\gamma \right\}. \tag{13}$$

Thereby, this will be the third way to obtain the dynamical critical exponent. This third estimate of z is independent of the values of the static critical exponents.

Moreover, the equilibrium overlap–overlap correlation function constrained to $q = 0$ was obtained by De Dominicis *et al* [9], and in six dimensions reads

$$C_{\mathrm{SRSB}}(x)|_{q=0} \sim \begin{cases} x^{-4} & \text{if } T = T_c \\ x^{-2} & \text{if } T < T_c \end{cases} \tag{14}$$

or in momenta space

$$C_{\mathrm{SRSB}}(p)|_{q=0} \sim \begin{cases} p^{-2} & \text{if } T = T_c \\ p^{-4} & \text{if } T < T_c. \end{cases} \tag{15}$$

The fact that the equilibrium correlation function $C(x)$ has a power-law decay also for $T < T_c$, implies that spin glasses are always critical in the glassy phase (i.e. below T_c) and therefore we can relate the off-equilibrium behaviour of the correlation function to the equilibrium critical exponents. Since the susceptibility is the integral of the correlation function

$$\chi = \int \mathrm{d}^6 x\, C(x) \tag{16}$$

and since in the region where the susceptibility grows (following a power law with time), the overlap remains very small, we can substitute equations (14) into equation (16) obtaining

$$\chi(t) \sim \begin{cases} t^{1/2} & \text{if } T = T_c \\ t^{4/z(T)} & \text{if } T < T_c. \end{cases} \tag{17}$$

If we take the limit $T \to T_c$ in the above equation we obtain that $h(T)$, the exponent of the growth of the susceptibility, must be discontinuous at the critical point (i.e. $h(T_c^-) = 1$ while $h(T_c^+) = \frac{1}{2}$).

Moreover, if we assume that $1/z(T)$ is proportional to the temperature (this happens in three and four dimensions [11, 12]) we must obtain a linear dependence on the temperature for $h(T)$ in the low-temperature phase.

3. Remanent magnetization

The first part of this work has been dedicated to the decay of the remanent magnetization.

We prepare the system with all the spins up ($M(t = 0) = 1$) and then we let it evolve towards equilibrium where, in the absence of any external field, no magnetization should remain. In the cold phase we expect the decay of the remanent magnetization to be algebraic (see equation (1)); in particular we are interested in the exponent of such a decay at the critical temperature (which hereafter will be called simply λ), to compare it with the same exponent of the SK model.

In the following subsections we report our calculation of the λ exponent in the MF approximation (see [13] for another calculation of the λ exponent in the spherical spin-glass model), together with the numerical verification and the estimates of such an exponent in the finite-dimensional cases ($d = 6$ and $d = 8$) and also for the SK model.

3.1. Analytical results in the SK model

To study analytically the dynamical properties of the SK model we define the following soft-spin Hamiltonian:

$$\beta \mathcal{H} = -\beta \sum_{ij} J_{ij} s_i s_j + \tfrac{1}{2} \sum_i s_i^2 + \tfrac{1}{4!} g \sum_i s_i^4 \tag{18}$$

where s_i ($i = 1, \ldots, N$), are one-dimensional real variables and J_{ij} is a symmetric matrix with independent elements following a Gaussian distribution with zero mean and variance proportional to $1/N$. From the random matrix theory [14] we know that, in the thermodynamic limit (i.e. N goes to infinity), the probability distribution for the eigenvalues of J_{ij} is given by the semicircle law:

$$\sigma(\mu) = \frac{1}{2\pi} (4 - \mu^2)^{1/2} \qquad |\mu| < 2. \tag{19}$$

A relaxation dynamics is introduced by means of the following Langevin equation:

$$\partial_t s_i(t) = -\frac{\partial(\beta \mathcal{H})}{\partial s_i(t)} + \xi_i(t) \tag{20}$$

where $\xi_i(t)$ are Gaussian noises with zero mean and variance $\langle \xi_i(t) \xi_j(t') \rangle = 2\delta_{ij} \delta(t - t')$. To study the dynamical evolution of this model, we diagonalize the J_{ij} matrix and we consider the dynamics of the projections $s^n(t)$ of the spins $s_i(t)$ on the eigenvector directions ψ_i^n (with eigenvalues μ_n), such that $s_i(t) = \sum_n s^n(t) \psi_i^n$, where $n = 1, \ldots, N$ is the eigenvector index. The properties of independence and orthonormality of the eigenvectors [14] allow us to define the following Langevin equation for the component s^n:

$$\partial_t s^n(t) = (\beta \mu_n - 1) s^n(t) - \frac{g}{3!} \sum_{\alpha\beta\gamma} s^\alpha(t) s^\beta(t) s^\gamma(t) \sum_i \psi_i^\alpha \psi_i^\beta \psi_i^\gamma \cdot \psi_i^n + \xi^n(t) \tag{21}$$

where $\xi^n(t)$ are the components of $\xi_i(t)$ in the eigenvectors basis.

As usual we take into account the nonlinear term perturbatively. The dynamical response function $G(t, t')$ is given by the Dyson equation:

$$G^{-1}(t, t') = G_0^{-1}(t, t') + \Sigma(t, t') \tag{22}$$

where $G_0^{-1}(t, t')$ is the inverse bare-response function and $\Sigma(t, t')$ is the self energy. In analogy with the equilibrium dynamics, we suppose that the leading term for large N and

large t is given by the Hartree–Fock approximation†:

$$\Sigma(t, t') = C(t, t)\delta(t - t') \tag{23}$$

where $C(t, t)$ is the dynamical autocorrelation:

$$C(t, t') = \overline{\langle s_i(t)s_i(t')\rangle} \tag{24}$$

evaluated at $t = t'$. We represent the average over the thermal noise as $\langle(\cdots)\rangle$, while $\overline{(\cdots)}$ indicates the average over the disorder as usual. With respect to the eigenvalues the autocorrelation function can be written as follows

$$C(t, t') = \int \mathrm{d}\mu\, \sigma(\mu)\langle s^\mu(t)s^\mu(t')\rangle. \tag{25}$$

The Langevin equation, (21), becomes

$$\partial_t s^n(t) = (\beta\mu_n - 1)s^n(t) - \frac{g}{2}C(t, t)s^n(t) + \xi^n(t). \tag{26}$$

The self-consistent solution of equation (26) is

$$s^n(t) = s^n(0)\mathrm{e}^{(\beta\mu_n - 1)t}\mathrm{e}^{-g/2\int_0^t \mathrm{d}t'\, C(t',t')} + \int_0^t \mathrm{d}t''\, \mathrm{e}^{(\beta\mu_n - 1)(t - t'')}\mathrm{e}^{-g/2\int_{t''}^t \mathrm{d}t'\, C(t',t')}\xi^n(t'') \tag{27}$$

where $t = 0$ is the initial time.

We want to analyse the evolution of the system at $T = T_c$ from a uniform initial condition: $s^n(0) = 1$, $\forall n$. From (27) we obtain the following self-consistent equation for $C(t, t)$:

$$C(t, t) = H^2(t) \int \mathrm{d}\mu\, \sigma(\mu)\mathrm{e}^{2(\beta\mu - 1)t} + 2 \int_0^t \mathrm{d}t'' \left(\frac{H^2(t)}{H^2(t'')}\right) \int \mathrm{d}\mu\, \sigma(\mu)\mathrm{e}^{2(\beta\mu - 1)(t - t'')} \tag{28}$$

where

$$H(t) = \mathrm{e}^{-g/2\int_0^t \mathrm{d}t'\, C(t',t')}. \tag{29}$$

Let us suppose for $H(t)$, at $T = T_c$, a time-dependent asymptotic behaviour ($t \to \infty$) like

$$H(t) \sim t^\rho \mathrm{e}^{-gt} \tag{30}$$

where ρ can be determined self-consistently from equation (28). This hypothesis implies for $C(t, t)$, at large t, the behaviour

$$C(t, t) \sim (2 + \Delta T_c) - \frac{a}{t} \tag{31}$$

where a is an appropriate constant. The critical temperature of the Hamiltonian (18) is given by $T_c = T_c^0 + \Delta T_c = 2 + \Delta T_c$ ($T_c^0 = 2$ is the critical temperature of (18) when $g = 0$) and a perturbative calculation gives $\Delta T_c = -2g$ so that $2\beta_c = 1 + g$ [15].

We recall that for $T \sim T_c$ the largest contribution to the dynamical relaxation of the spins comes from the region of the maximum eigenvalue, $\mu = 2$.

At the critical point, the first term on the r.h.s. of equation (28) scales like a power law $t^{-3/2 + 2\rho}$. To be consistent with the hypothesis (30) and (31) we should have $\rho \leqslant \frac{1}{4}$.

Now we have to estimate the second term, which is proportional to:

$$2 \int_0^t \mathrm{d}t'' \int \mathrm{d}\mu\, \sigma(\mu)\frac{t^{2\rho}}{t''^{2\rho}}\mathrm{e}^{-2\beta_c(2 - \mu)(t - t'')}. \tag{32}$$

† We have verified that the results obtained are consistent with this assumption.
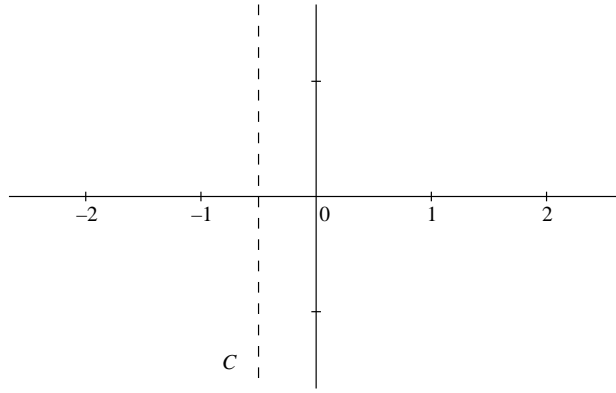
Figure 1. The integration path.

Let us consider $t' = t - t''$ and we define the exponential as an integral in the complex plane,

$$\mathrm{e}^{-2\beta_c(2-\mu)t'} = \sum_k \frac{(-1)^k}{k!}[2\beta_c(2-\mu)t']^k = \int_{\mathcal{C}} \frac{\mathrm{d}s}{2\pi\mathrm{i}} \Gamma(-s)[2\beta_c(2-\mu)t']^s \quad (33)$$

where $\mathcal{C}$ is the path shown in figure 1 (i.e. $s = s_0 + ir$, where $r \in \mathcal{R}$, and s_0 is an arbitrary real number in $(-1, 0)$) $\Gamma(s)$ is the Euler gamma function. We obtain:

$$2 \int_{\mathcal{C}} \frac{\mathrm{d}s}{2\pi\mathrm{i}} \int_0^t \mathrm{d}t' \, \Gamma(-s) \frac{t^{2\rho}}{(t-t')^{2\rho}} t'^s \int \mathrm{d}\mu \, \sigma(\mu)(2\beta_c)^s (2-\mu)^s. \quad (34)$$

After the integration over t' and μ we can write:

$$\frac{8}{\sqrt{\pi}} \int_{\mathcal{C}} \frac{\mathrm{d}s}{2\pi\mathrm{i}} \Gamma(-s)t^{1+s} \frac{\Gamma(s+1)\Gamma(1-2\rho)}{\Gamma(s-2\rho+2)} 4^s (2\beta_c)^s \frac{\Gamma(s+\frac{3}{2})}{\Gamma(3+s)}. \quad (35)$$

To evaluate the integral (35) we analytically continue the function on the left of the path $\mathcal{C}$, i.e. in the region where $\mathrm{Re}\, s < s_0$. Thereby, we have to consider the residues of the poles in this region. The residue of the pole at $s = -1$ gives the constant contribution to the autocorrelation function $C(t, t)$ while the time-dependent behaviour, for large t, is determined by the value of ρ. In fact, for $\rho = \frac{1}{4}$, $\Gamma(s+\frac{3}{2})$ simplifies to $\Gamma(s-2\rho+2)$, and, for large t, the leading behaviour of $C(t, t)$ comes from the residue of the pole at $s = -2$:

$$C(t, t) \sim \text{constant} + t^{-1} \quad (36)$$

consistent with the hypothesis (30) and (31).

For $\rho \neq \frac{1}{4}$, on the contrary, we cannot cancel the pole at $s = -\frac{3}{2}$ and we should obtain

$$C(t, t) \sim \text{constant} + t^{-1/2} \quad (37)$$

in contrast to the previous hypothesis. Thus the only consistent solution for $H(t) \sim t^\rho \mathrm{e}^{-t}$ is $\rho = \frac{1}{4}$.

Another method of obtaining the ρ exponent is solving equation (28) in Laplace transform space. In terms of the function $g(t)$

$$g(t) \equiv \mathrm{e}^{-2gt} \frac{C(t, t)}{\Gamma^2(t)} \quad (38)$$

equation (28) at $T = T_c$ becomes:

$$g(t) = \int d\mu\, \sigma(\mu)e^{-2\beta_c(2-\mu)t} + 2\int_0^t dt'' \frac{g(t'')}{C(t'',t'')} \int d\mu\, \sigma(\mu)e^{-2\beta_c(2-\mu)(t-t'')}. \tag{39}$$

By using the asymptotic form (31) of $C(t,t)$, we obtain the following asymptotic equation for the Laplace transform of $g(t)$, that we will denote $\tilde{g}(s)$:

$$\tilde{g}(s) = \int d\mu\, \sigma(\mu) \left[\frac{1}{s + 2\beta_c(2-\mu)} \right]$$
$$+ \int d\mu\, \sigma(\mu) \left[\frac{1}{s + 2\beta_c(2-\mu)} \right] \left[\left(1 - \frac{\Delta T_c}{2} \right) \tilde{g}(s) + \frac{a}{2} \int_s^\infty dx\, \tilde{g}(x) \right]. \tag{40}$$

By averaging over the eigenvalue distribution we obtain:

$$\tilde{g}(s) = \left(\frac{1}{2\beta_c} - \frac{\sqrt{2s}}{4\beta_c^{3/2}} \right) + \left(\frac{1}{2\beta_c} - \frac{\sqrt{2s}}{4\beta_c^{3/2}} \right)$$
$$\times \left[\left(1 - \frac{\Delta T_c}{2} \right) \tilde{g}(s) + \frac{a}{2}(1 - \Delta T_c) \int_s^\infty dx\, \tilde{g}(x) \right]. \tag{41}$$

By remembering that $\beta_c = 1/(2 + \Delta T_c)$, we can expand the previous equation in ΔT_c. We will also assume that in the limit $s \to 0$; $\int_s^\infty dx\, \tilde{g}(x)$ is negligible with respect to $\tilde{g}(s)$, and we finally obtain

$$\tilde{g}(s) \sim \frac{1}{\sqrt{s}} + \mathrm{O}(1). \tag{42}$$

Thus, for $t \to \infty$, $g(t) \sim 1/t^{1/2}$ and from (38) we obtain $\rho = \frac{1}{4}$. This solution implies that $\int_s^\infty dx\, \tilde{g}(x) \ll \tilde{g}(s)$.

At this point, we can determine the decay rate of the correlation between the system at time t and the system at $t = 0$, i.e. the scaling decay of the remanent magnetization:

$$M(t) = C(t,0) = \overline{\langle s_i(t) \rangle} = \int d\mu\, \sigma(\mu)\langle s_\mu(t) \rangle \tag{43}$$

$$= \int d\mu\, \sigma(\mu)H(t)e^{(\beta\mu-1)t} \sim \frac{1}{t^{3/2}}t^{1/4} \sim t^{-5/4}. \tag{44}$$

Thus, the analytical prediction for the exponent λ, defined by $M(t) \sim t^{-\lambda}$, is, in the MF limit, $\lambda = \frac{5}{4}$.

This result is quite different from the one obtained in the spherical model at $T = T_c$ where $\lambda = \frac{3}{4}$ [13].

3.2. Numerical results in infinite (SK model) dimensions

For a numerical confirmation of this result we have simulated three SK models at criticality ($T_c = 1$) of sizes $N = 480, 992, 2016$ with number of samples of $10\,000$, 5000 and 1000 respectively, obtaining three estimates of the λ_{MF} exponent all compatible with the theoretical prediction. Since the data for the remanent magnetization contain non-evident finite-size effects, in figure 2 we have plotted the data averaged over all the simulated samples. The observable that we have measured is $M(t, t_w = 3)$ defined in equation (4), which follows the same decay of $M(t)$ but has some advantages as will be explained below. The line in figure 2 is the best power fit which gives $\lambda_{\mathrm{MF}} = 1.22 \pm 0.02$.

We have repeated this numerical calculation for a temperature below the critical one ($T = 0.8\,T_c$) and sizes $N = 480, 992, 2016, 4064$. In this case we expect that the remanent
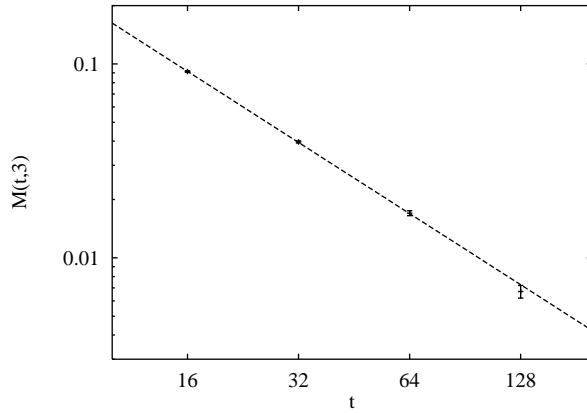
Figure 2. Remnant magnetization in the SK model at $T = T_c$. The line is the best power fit which gives an exponent $\lambda_{\mathrm{MF}} = 1.22 \pm 0.02$.
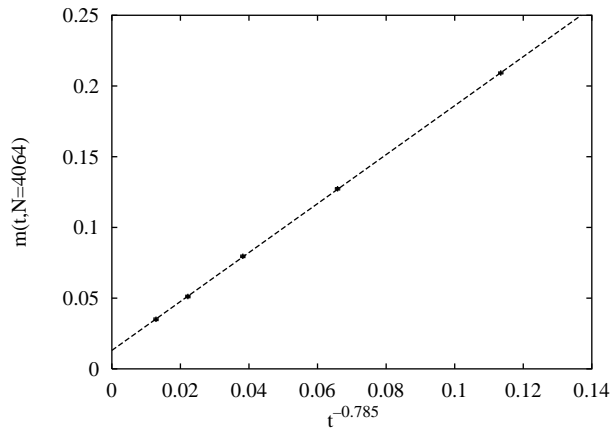
Figure 3. Remnant magnetization in the SK model at $T = 0.8\,T_c$ plotted versus $t^{-\lambda(T)}$, to make more evident the finite-size effect ($m(t = \infty) \neq 0$). The line is the linear fit.

magnetization tends to a non-zero asymptotic value due to the finite size of the system. So we have fitted the data for $M(t, t_w = 3)$ with the following formula

$$m(t, N) = m_\infty(N) + At^{-\lambda(T)} \tag{45}$$

where we let λ depend on the temperature. Via a preliminary three-parameter fit we have estimated $\lambda = 0.785(10)$ and found no systematic dependence on the lattice size. Then fixing the value of λ to this previously found value, we extrapolated the value of $m_\infty(N)$ by using a simple linear fit, such as the one plotted in figure 3.

Using the values of $m_\infty(N)$ found by the previous analysis we were able to fit them to a power law of the system size: $m_\infty(N) \propto N^{-0.25(1)}$. The data with the best fit are reported in a double-log scale in figure 4 (see [16] for a detailed study).

Assuming a linear dependence of the exponent $\lambda(T)$ with the temperature, which has been observed in [16, 17] for the SK model and in [18] for a spin-glass system on quenched ϕ^3 graphs (which should behave like a mean-field SK model), and from the fact that $\lambda(T = 0.8) \simeq 0.8$, we obtain that the λ critical exponent as a function of the temperature
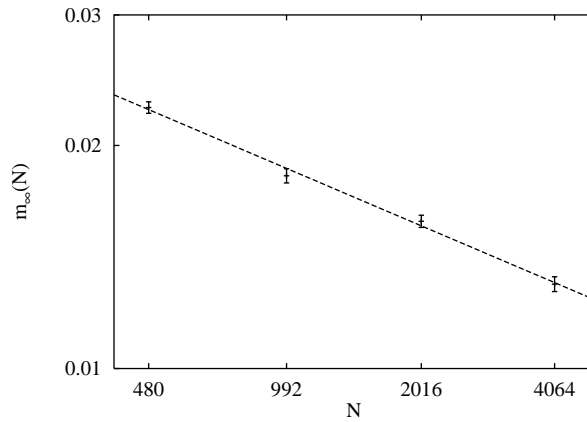
Figure 4. $m_\infty(N)$ versus N in the SK model at $T = 0.8\ T_c$. The line is the best power fit.

is discontinuous at the critical point (i.e. $\lambda(T_c^-) \simeq 1$ while $\lambda(T_c^+) = \frac{5}{4}$).

3.3. Numerical estimate in $d = 6$ and $d = 8$

The measurement of the decay rate of the remanent magnetization is not easy because although we know that $M(t = 0) = 1$ we try to fit the $M(t)$ data with a power law which diverges at $t = 0$. This effect is evident in a log–log scale where a power fit behaves like a straight line, while the $M(t)$ data tends to the value 1 when $\ln t \to -\infty$; in such a situation we have to discard the first data points to be sure we are measuring the asymptotic behaviour. Unfortunately the useless data have the smaller relative error, while the data fitted are affected by a greater statistical indetermination which makes the estimate of λ more difficult.

One possible way to overcome this source of error is to measure some other observable that has the same behaviour of $M(t)$, but with a stronger and less fluctuating signal. Starting with all the spins up, the magnetization at time t is just the overlap between the configuration at time t and the initial one. If we measure the overlap between the configuration at time t and one at a fixed small time ($t_w = 3$ in our case), we expect that $M(t, t_w)$ behaves like $M(t)$, with similar statistical fluctuations, but with a signal 10 times greater.

The results of the simulations of the SG model in six dimensions can be found in figure 5 where we have plotted $M(t, t_w = 3)$ versus the simulation time t; the line is the best power fit which gives an exponent $\lambda = 0.995 \pm 0.005$. This value is compatible with 1, but not with the MF value $\lambda_{MF} = \frac{5}{4}$.

As explained in the introduction we believe that the upper critical dimension becomes $d_u = 8$ for such quantities linked to a magnetic field. In this case we start the simulation with the system totally magnetized, as if it was feeling an infinitely strong magnetic field, so the remanent magnetization may be one such quantity.

For this reason we have done some simulations of the Ising spin-glass model in $d = 8$ (again with the couplings $J = \pm 1$) to see if we recover the MF behaviour of the remanent magnetization.

The critical temperature in $d = 8$ that we have used was extrapolated from the critical temperatures in d=3 [19], 4 [20] and 6 [6]. In the limit of $d \to \infty$ the critical temperature diverges like $T_c(d) \simeq \sqrt{2d}$. Moreover, in the Bethe–Peierls approximation, there is an
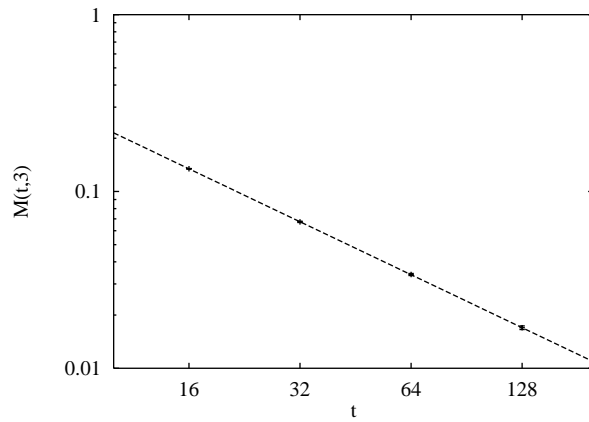
Figure 5. Remnant magnetization in $d = 6$ at $T = T_c$ together with the best power fit, which gives an exponent $\lambda = 0.995 \pm 0.005$.

exact formula for the critical temperature [21, 22]

$$(2d - 1)\tanh^2(\beta_c) = 1. \tag{46}$$

We have used this formula, which turns out to be valid in the $d \to \infty$ limit, as a starting point adding it some terms which may mimic the finite dimensions corrections. In particular we have substitute the r.h.s. of equation (46) with a fourth-order polynomial in $1/d$ (the term of zeroth order being always 1) and we tried to fit the known critical temperatures by fixing two terms of the polynomial to zero and leaving free the coefficients of the other two terms. Among the six possible choices we have selected the one with the smallest value of χ^2, which is

$$(2d - 1)\tanh^2(\beta_c) = 1 + \frac{B}{d^2} + \frac{D}{d^4} \tag{47}$$

with $B = 0.95 \pm 0.14$ and $D = 117 \pm 4$. With this fit we estimate the critical temperature for the eight-dimensional model as $\beta_c(d = 8) = 0.270 \pm 0.001$. The error reported is an underestimate of the real one because there are systematic deviations due to the arbitrary choice of the fitting function.

We have also repeated the analysis looking at the quantity $T_c^2/(2d - 1)$, which takes values in the range $[0, 1]$. Knowing that in the $d \to \infty$ limit

$$\frac{T_c^2}{2d - 1} = 1 \tag{48}$$

we have tried to fit the critical temperatures by adding to the r.h.s. of equation (48) a polynomial in $1/d$, obtaining as the best interpolation, reported in figure 6,

$$\frac{T_c^2}{2d - 1} = 1 - 5.16(26)\frac{1}{d^2} - 5(1)\frac{1}{d^3}. \tag{49}$$

From the plotted fit we obtain an estimate of $\beta_c(d = 8) = 0.270 \pm 0.001$. This error is too small because systematic deviations due to the arbitrary choice of the fitting function are not taken into account.

Moreover the estimates of $\beta_c(d = 8)$ obtained with different interpolations are all in the range $[0.260, 0.270]$ and we consider that the true critical temperature is within very good probability in this range; in fact, as one can see in figure 6, the value of $\beta_c(d = 8)$ is
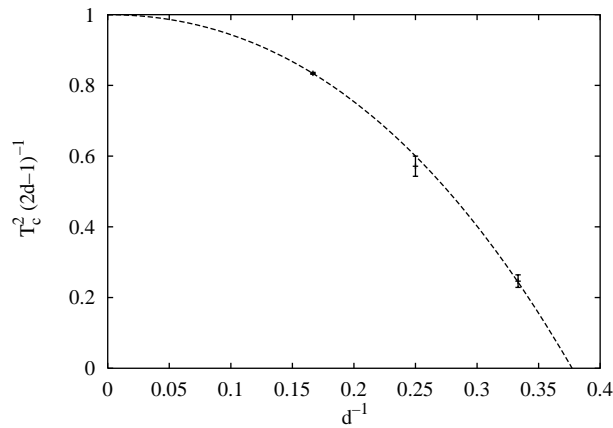
Figure 6. Critical temperatures of the SG model against the dimensionality. The line is a polynomial fit as described in the text.
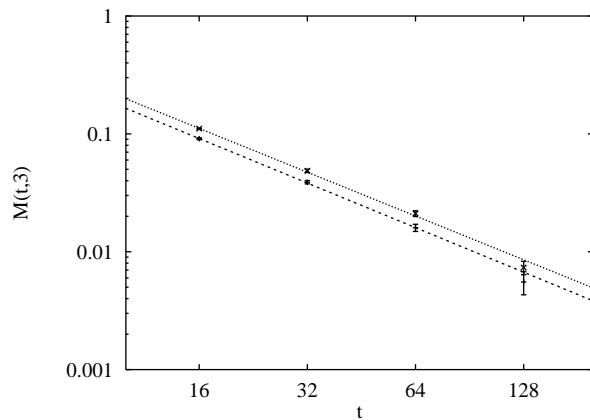

Figure 7. Remnant magnetization in $d = 8$ at two temperatures very near to the critical one. The lines are the power fits which give exponents compatibles with the MF predictions $\lambda_{MF} = 5/4$.

strongly dependent on the value of $\beta_c(d = 6)$, which is known with high accuracy, and on the way $\beta_c(d)$ tends to zero as the dimensionality is increased.

For example, if we assume that the successive improvements of the Bethe–Peierls approximation tend to increase the value of $\beta_c(d)$ for each d, then formula (46) will give a lower bound for the inverse critical temperature; in $d = 8$ this lower bound reads $\beta_c(d = 8) > 0.264$.

From figure 6 we can also get further important information: the point where the fitting function crosses the d^{-1}-axis may give us an estimate of the lower critical dimension, which is $d_l \simeq 2.65$.

In figure 7 we have plotted the data, with the best power fits, of the remanent magnetization in $d = 8$ at temperature $\beta = 0.260$ and 0.270. From the fits we get the exponents $\lambda(\beta = 0.260) = 1.256 \pm 0.08$ and $\lambda(\beta = 0.270) = 1.235 \pm 0.013$, which are both compatible with the MF result ($\lambda_{MF} = 5/4$).
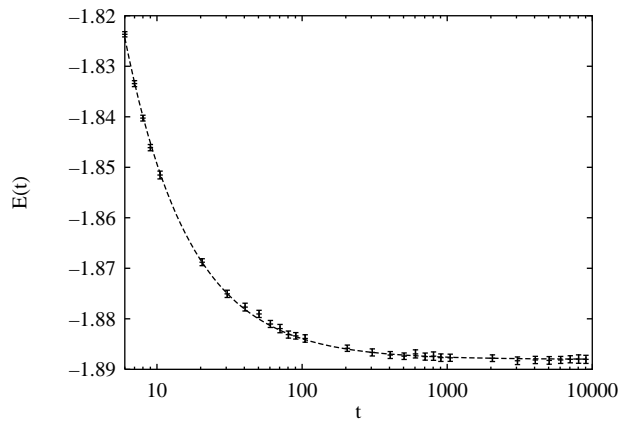
Figure 8. Energy decay in a system of volume 10^6 at the critical temperature. The curve plotted is the best power fit, which gives a value for the exponent $\delta = -0.98 \pm 0.01$ compatible with the MF one $\delta_{\mathrm{MF}} = -1$.

4. Results in $d = 6$

The major part of the simulation work has been done at the critical temperature, chosen as the weighted mean between the one found by Wang and Young [6] ($T_c = 3.035 \pm 0.01$) and the one calculated by series expansion [23] ($T_c = 3.027 \pm 0.005$): $\beta_c = 0.3302 \pm 0.0005$. In particular we have tested that the exponents measured do not vary significantly if the temperature is changed by an amount of the order of the uncertainty on T_c. To this purpose we have simulated the same system (of volume 8^6) at the inverse temperatures $\beta_1 = 0.330$ and $\beta_2 = 0.331$, checking that the dynamics were compatible.

Having verified that, for the range of time and sizes we have used, the exponents we are interested in do not depend on the precise choice of T_c, we have decided to run all the subsequent simulations at $\beta_c = 0.330$. At the critical point we have simulated more than 200 samples of size 8^6, 13 samples of size 10^6 and also 106 samples of an asymmetric lattice 12×8^5. The final number of samples may appear too small to average over the disorder; in fact we have used data mainly from the 8^6 systems to calculate the moments of the distribution of the overlaps. The data from the bigger systems have been used to measure almost-self-averaging quantities such as energy whose fluctuations are very small considering that we are working with a system with a million spins.

The results are shown in figure 8 for the energy decay and in figure 9 for the nonlinear susceptibility growth.

We have tried to fit the energy decay both to a power law ($E(t) = E_\infty + At^{-\delta}$) and to a logarithmic law ($E(t) = E_\infty + A[\ln(t/\tau)]^{-\delta}$). We are interested in the asymptotic behaviour of the decay; then we fit the data in the range $t \in [t_{\min}, \infty)$ for various choices of $t_{\min}$ and we expect that the parameters of the fit converge quickly when we increase $t_{\min}$. The impossibility of fitting all the data with a single law (for $t < 6$) is due to the existence of an initial short time regime of a few steps during which the dynamic does not yet follow the asymptotic behaviour. We find that the logarithmic law does not describe well the data because, even if it has more adjustable parameters, the best values of the parameters depend strongly on $t_{\min}$, they are very correlated and they tend towards unphysical values. On the other hand we find that fitting with the power law the values of the parameters E_∞, A and δ converge to a stable value, with $t_{\min}$ of order of few Monte Carlo steps (MCS). In
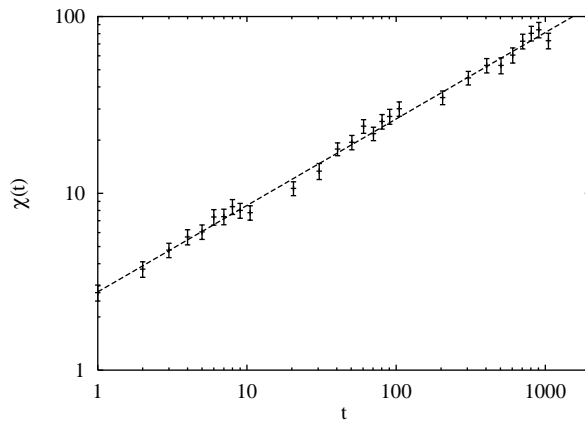
Figure 9. Susceptibility growth in systems of size 8^6 at $T = T_c$. The line is the best power fit which gives an exponent $h = 0.49 \pm 0.01$ in agreement with the MF value $h_{MF} = \frac{1}{2}$.

figure 8 we plot the power fit obtained with $t_{min} = 6$ (this is the lowest value for which the fit satisfies the χ^2 test); the best parameters are: $E_\infty = -1.8880 \pm 0.0001$, $A = 0.37 \pm 0.01$ and $\delta = -0.98 \pm 0.01$. We note that the decay exponent is compatible with the mean field value ($\delta_{MF} = -1$).

The line plotted in figure 9 is the best power fit to the susceptibility data. We have to be careful when we try to interpolate these data with a power law because we know that the susceptibility growth follows a power law only in a limited time range; in fact at the beginning of the simulation the dynamics need some time to reach the asymptotic regime† and then because of the finite size of the system they have to converge to some finite value, i.e. the data of figure 9 have to converge to a plateau. These two effects may induce systematic deviations in the estimate of the h exponent: $\chi(t) \propto t^h$. In our case the first transient is almost absent thanks to the sufficiently high temperature and the problems arising from the finite-size effects have been solved by fitting the $\chi(t)$ data only in a limited time range far away from the plateau (estimated in a previous longer run). The line reported in figure 9 is the best power-law fit to the $\chi(t)$ data (209 samples of an 8^6 system), which gives an estimate of the dynamical exponent $h = 0.49 \pm 0.01$ which is compatible with the MF value ($h_{MF} = \frac{1}{2}$).

We also show in figure 10 the results (obtained on the $8^5 \times 12$ lattice) for the h exponent in the low-temperature phase ($T/T_c = 0.5, 0.625, 0.75, 0.875$). We also plot in this figure the value obtained at T_c ($h = 0.49$). It is clear that $h(T)$ is a discontinuous function at the critical point and that the limit from below, assuming a linear behaviour, ($h(T_c^-) \simeq 0.9$) is almost twice the value of $h(T_c^+) = 0.5$, in very good agreement with the correlation functions (propagators), which are restricted to the $q = 0$ ergodic component, found by De Dominicis *et al* [9]. The quite small discrepancy can be due to the crossover between the two regimes in a finite lattice or due to logarithmic corrections.

Moreover we can see that the dependence of this exponent is well described by a linear law of the temperature, according to a $z(T)$ proportional to $1/T$.

Finally, we studied the spatial correlations by the following technique (already used with success for the data analysis in three and four dimensions [11, 12]). We expect a functional

---

† This initial time increases when the temperature is lowered.
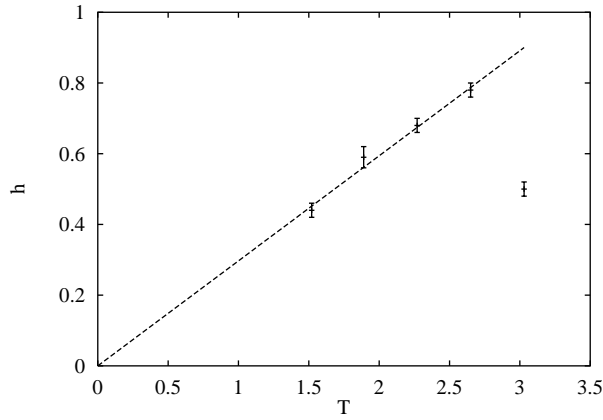
Figure 10. Behaviour of the exponent $h(T)$. Note that the linear fit which describes well the data in the cold region, when $T \to T_c$ tends to a value almost twice the one measured just at $T = T_c$. This confirms that the propagators (which are restricted to the $q = 0$ ergodic component) at and below T_c are proportional to p^{-2} and to p^{-4} respectively.

dependence for this correlation function of the form

$$G(t, x) = \frac{a(T)}{x^\alpha} \exp\left\{ -\left(\frac{x}{\xi(T, t)} \right)^\gamma \right\} \tag{50}$$

where, as usual, $\xi(T, t) \propto t^{1/z(T)}$ is the dynamical correlation length. For each value of the distance we fit the data of the $q - q$ correlation function to the formula

$$G(x, t) = G_\infty(x) \exp[A(x)t^{-B}] \qquad \forall \text{ fixed } x \tag{51}$$

and we verify that the value of the B parameter is almost independent from x and then we fix it during the following study. The dynamical exponent can be expressed as the ratio $z = \gamma/B$, where γ may be estimated by the power-law fit $A(x) \propto x^\gamma$. This method yields our third estimate $z = 4.2 \pm 0.2$ which is again compatible with the MF value. In figure 11 we have plotted $\ln G(x = 2, t)$ versus t, together with the best fit (equation (51)).

In the infinite time limit the function $G(x, t)$ converges to $G_\infty(x)$ which must give information on the $q - q$ correlation function at zero overlap, calculated for the SK model by De Dominicis *et al* [9]. They found that $G_{q=0}(x) \propto x^{-4}$ at the critical temperature.

By our simulation we find the $G_\infty(x)$ plotted in figure 12 together with the best power fit in the range $x \in [2, 5]$. We note that the point in $x = 1$ if far away from the fit because for $\ln(x) \to -\infty$ the data must converge to 1 (by definition $G(x = 0) = 1$) while the power fit diverges. Anyway we are interested in the asymptotic behaviour which seems to be well described by a power law, $G_\infty(x) \propto x^{-\alpha}$ with an exponent $\alpha = 4.2 \pm 0.1$, in agreement with the MF result previously cited.

5. Conclusions

We have calculated analytically in the MF approximation the exponent of the remanent magnetization and we obtain numerical results that confirm that for this observable the upper critical dimension is eight and not six.

For the first time we have numerically calculated the dynamical critical exponents in six dimensions in three different ways, all compatible within the statistical error.
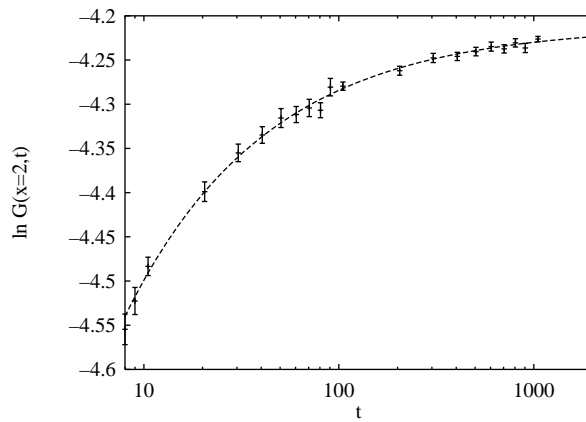
Figure 11. $\ln G(x = 2, t)$ versus t at the critical temperature. The line is the best power fit whose asymptotic value is $\ln G_\infty(x = 2)$.
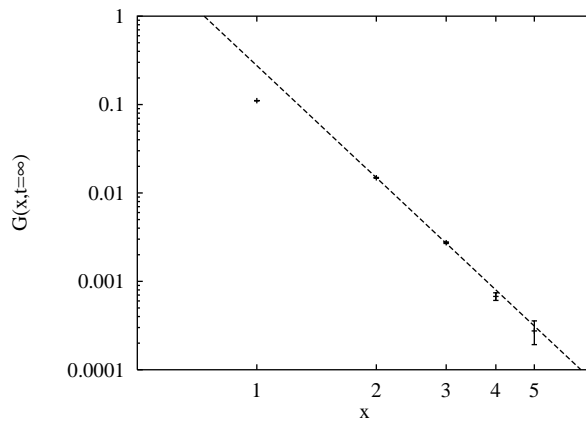
Figure 12. $G_\infty(x)$ at the critical point. The line is the best power fit to the data with $x > 1$, which gives an exponent $\alpha = 4.2 \pm 0.1$.

Thanks to the previous results we can also check the static critical exponents (for instance getting the z value obtained from the scaling of the $q - q$ correlation function), and we obtain values that agree very well with the static critical exponents and the critical temperature found in the literature [6].

Moreover, by monitoring the growth of the nonlinear susceptibility in the spin-glass phase, we have shown numerical evidence favouring a p^{-4} propagator, constrained to the $q = 0$ ergodic component, according with the analytical results obtained assuming spontaneously broken replica symmetry. This numerical result is a further check that it is possible to have spontaneously broken replica symmetry in finite dimensions.

We plan in the future to extend this work to the five-dimensional Ising spin glass.

Acknowledgments

References

[1] Parisi G 1994 *Field Theory, Disorder and Simulations* (Singapore: World Scientific)
[2] Newman C M and Stein D L 1996 *Phys. Rev. Lett.* **76** 515
[3] Granberg P, Svedlindh P, Nordblad P, Lundgren L and Chen H S 1987 *Phys. Rev.* B **35** 2075
[4] Kisker J, Santen L, Schreckenberg M and Rieger H 1996 *Phys. Rev.* B **53** 6418
[5] Fisher D and Sompolinsky H 1985 *Phys. Rev. Lett.* **54** 1063
[6] Wang J and Young A P 1993 *J. Phys. A: Math. Gen.* **26** 1063
[7] Ogielski A T 1985 *Phys. Rev.* B **32** 7384
[8] Parisi G and Ranieri P 1997 *Preprint* cond-mat/9701160
[9] De Dominicis C, Kondor I and Temesvari T 1993 *Int. J. Mod. Phys.* B **7** 986
[10] Rieger H 1995 *Annual Reviews of Computational Physics II* (Singapore: World Scientific) p 295
    See also Marinari E, Parisi G and Ruiz-Lorenzo J J 1997 *Spin Glasses and Random Fields* ed P Young
        (Singapore: World Scientific) to appear, also available as *Preprint* cond-mat/9701016
[11] Marinari E, Parisi G, Ruiz-Lorenzo J J and Ritort F 1996 *Phys. Rev. Lett.* **76** 843
[12] Parisi G, Ricci-Tersenghi F and Ruiz-Lorenzo J J 1996 *J. Phys. A: Math. Gen.* **29** 7943
[13] Cugliandolo L F and Dean D S 1995 *J. Phys. A: Math. Gen.* **28** 4213
[14] Metha M L 1967 *Random Matrices* (New York: Academic)
[15] Ranieri P 1996 *J. Phys. I France* **6** 807
[16] Marinari E, Parisi G and Rossetti D 1997 *Preprint* cond-mat/9708025
[17] Parisi G and Ritort F 1993 *J. Phys. I France* **3** 969
[18] Baillie C, Johnston D A, Marinari E and Naitza C 1996 *J. Phys. A: Math. Gen.* **29** 6683
[19] Kawashima N and Young A P 1996 *Phys. Rev.* B **53** R484
[20] Badoni D, Ciria J C, Parisi G, Pech J, Ritort F and Ruiz-Lorenzo J J 1993 *Europhys. Lett.* **21** 495
    Young P 1996 Private communication
[21] Mèzard M and Parisi G 1987 *Europhys. Lett.* **3** 1067
[22] Serva M and Paladin G 1996 *Phys. Rev.* E **54** 4637
[23] Klein L, Adler J, Aharony A, Harris A and Meir Y 1991 *Phys. Rev.* B **43** 11 249